Journal of Engineering Research and Reports

20(4): 117-130, 2021; Article no.JERR.66180
ISSN: 2582-2926

Dynamic Analysis of Fatigue Life Prediction on the Shafts of a Modern Cassava Peeling Machine for Safe and Economic Use

Pondi Pius Eddy[1], Nwigbo Solomon Chuka[1], Obende Eziekel Omeiza[1], Olisakwe Henry Chukwuemeka[1], Chikelu Okechukwu Peter[1] and Azaka Onyemazuwa Andrew[1*]

[1]Department of Mechanical Engineering, Nnamdi Azikiwe University, Awka, Anambra State, Nigeria.

Authors' contributions

This work was carried out in collaboration among all authors. Authors NSC, PPE and AOA designed the study, performed the statistical analysis, wrote the protocol and wrote the first draft of the manuscript. Authors OEO and COP managed the analyses of the study. Author OHC managed the literature searches. All authors read and approved the final manuscript.

Article Information

DOI: 10.9734/JERR/2021/v20i417301
Editor(s):
(1) Dr. David Armando Contreras-Solorio, Autonomous University of Zacatecas, Mexico.
Reviewers:
(1) Zhonggang Xiong, Guilin University of Aerospace Technology, China.
(2) Fu Zhang, Henan University of Science and Technology, China.
Complete Peer review History: http://www.sdiarticle4.com/review-history/66180

Original Research Article

Received 08 January 2021
Accepted 09 March 2021
Published 27 March 2021

ABSTRACT

The durability of a machine structure is based on its mechanical performance through its entire service life. To avoid structural failures in machines, it is a standard design practice that machines be analyzed based on the types of loading (static and fatigue) associated with it in order to design safe and dependable machine structures. These types of analyses are performed with the purpose of estimating the behavior of the mechanical parts under specific operational conditions. The aim of this research is to investigate the effect of different loading to the maximum load on the redesigned shafts of an existing cassava peeling machine capable of peeling at least one (10) tons of cassava tubers with different weight, size or shape per day to ascertain the effects on the bending moment, shear force, deflection angle, shear stress and bending stress, and evaluate if there is need to reduce or increase the thickness of the shafts to a standard considered to be safe and economical. The three shafts of the cassava peeling machine have been carefully analyzed to check for their fatigue life under different loading conditions. From the analysis, with stress values of 48.640MPa, 49.1289MPa, 3.06089MPa and shaft diameter values of 34.6799mm, 34.7955mm,

**Corresponding author: Email: oa.azaka@unizik.edu.ng, azakaonyemazuwa@gmail.com;*

13.7941mm evaluated from the reduced stress diagrams and ideal diameter diagrams for abrasive cylinder shaft, peeling cylinder shaft, and retainer shaft respectively, gave positive results because none of stress values were greater than reduced stresses (calculated stress value from Tresca's theory) on the respective shafts. Therefore, a standard steel shaft of 35mm diameter is appropriate for manufacturing of the machine and also safe and economical.

Keywords: Design; machine shaft; stress analysis; fatigue life prediction.

1. INTRODUCTION

Poor design can cause regular breakdown of machines. To avoid regular failure of machine parts, it is a good practice to subject most essential parts of a machine to failure check after design. This is to prevent frequent failure of the components parts and increase the performance of the structure and machine life. It will also enable quality assurance engineers, reliability engineers, design engineers, etc. in the development of quality and efficient products [1].

As Nigeria props up her desire to be a major exporter of cassava and its by-products to the international market being the world's leading producer of cassava [2,3] (FAO, 2008), the need for proper design of an efficient and reliable cassava peeling machine for safe and economic use cannot be overemphasized. Due to the poor storage characteristics of cassava tuber in its unprocessed state, and unavailability of an efficient and reliable peeling machines, it is necessary to process fresh cassava tubers into a form that is more easily stored in order to minimize deterioration and losses with a view to delivering good quality products obtainable at the lowest production cost as well as the shortest production time. In doing this, equilibrium balance between food supply and population growth would be maintained, as food losses during production time would be reduced to the barest minimum.

A more recent cassava peeling machine which has proved to be more efficient than other existing machines, but experiences consistent shaft deformation during operations has been chosen for this study (shaft redesigning). The shafts of the machine are to be redesigned to ensure it is capable of peeling at least ten (10) tons of cassava tubers with different weight, size or shape per day. The machine which requires upgrade was designed in the department of mechanical engineering, Nnamdi Azikiwe University, Awka, Nigeria, [4] and is currently used in commercial cassava processing facilities in south eastern Nigeria. But due to its constant shaft deformation when operating on its design capacity (5 tons), the need for its upgrade (shaft redesigning and tonnage capacity) is the aim pursued in this work.

The cultivation of cassava requires minimal input, but the processing of cassava roots is labour-intensive requiring mechanization in order to meet up with its current demand. Processing of root crops is essential to reduce its perish-ability and therefore a very little portion is consumed as fresh products. This is because cassava roots deteriorates within few days after harvest with the rate of deterioration varying between cassava varieties.

Cassava can be processed into several storage products in Nigeria as listed; flour, garri, lafun, fufu, pupuru, abacha, chips/pellets and other industrial products like starch and alcohol. Processing cassava into storable and economic products involves different combinations and sequence of two or more of a number of processing steps which includes; washing, peeling, splitting, pulping, steaming, water expressing/dewatering, fermentation, pulverizing, sieving or sifting of mash, roasting or frying and sun or smoke drying. The operations involved in the preliminary processing of various forms of cassava include washing, peeling and size-reduction generally. Peeling which is defined as "to strip off the skin" is an important operation in the processing of any tuber or root crop. Traditionally, the operation of peeling is done manually using a knife to remove the thin outer layers of the tuber. This is often time wasting and energy consuming which invariably leads to low productivity. There is therefore the need for this operation to be done mechanically.

A number of cassava peeling machines have been developed and reported in literatures; Ejovo et al. [5], Ohwovoriole et al. [6], Odigboh [7], Odigboh [8], Ariavie et al. [9], Adetan et al [10], Olukunle et al. [11], Agbetoye et al. [12], Akande et al. [13], Olukunle et al. [14], Kolawole et al. [15]. Most of these machines are still in use in most parts of the country, but they are not as efficient as the Cassava peeling machine developed by Pondi et al. [4]. Hence pondi et al

which has proved to be more efficient and recent was chosen for upgrade and analysis, to provide reliable data for design engineers.

The durability of a machine structure is based on its mechanical performance through its entire service life. To avoid structural failures in machines which is primarily due to the static and dynamic loads acting on the machine during operations, it is a standard design practice that the machine be analyzed based on the types of loading (static and fatigue) associated with it in order to design safe and dependable machine structures. These types of analyses are performed with the purpose of estimating the behavior of the mechanical parts under specific operational conditions [1]. In the past, these analyses were performed through tests that were carried out on prototypes of the product, which meant an increase on the time needed to develop the product, as well as an increase on the related costs. However, technological advancements have allowed developers and engineers to depend upon computational tools to carry out these tests virtually via the Finite Elements Method (FEM).

The aim of this research is to redesign the shafts and increase the tonnage capacity of an existing cassava peeling machine that has failed consistently when subject to different loading conditions during operations. The new designed shafts would be subjected to different loading to the maximum load to ascertain the effects of the loads on the bending moment, shear force, deflection angle, shear stress and bending stress which resulted to consistent failure of the previous shafts, and evaluate if there is need to reduce or increase the thickness of the shafts to a standard considered to be safe and economical.

2. DESIGN AND METHODOLOGY

The terms of reference are modeling, dynamic simulation and performance analysis of the shafts of a portable, low speed (50 rpm -100 rpm) cassava peeling machine. The design of the machine shafts was done using conventional methods and other computer application software (Autodesk inventor software).

2.1 Design Consideration

In order to achieve high efficiency and reliability, the machine was designed based on the following considerations:

- It should be cheap and within the purchasing capacity of local farmers.
- It should be able to peel different varieties, shapes and sizes of cassava and have reasonable peeling efficiency.
- It should be fabricated from readily available materials most of which should be locally sourced.
- During use, it should be able to reduce labour input in traditional method of peeling.
- It should have high capacity compared to manual operations.

2.2 Components of the Peeling Machine

The cassava peeling machine has the following as its components [4]:

- **The transmission system:** This comprises of the electric motor, speed reducer, universal/knuckle joint, pulleys, v-belt, gears, bearings and shafts.
- **The peeling chamber:** this comprises the peeling cylinder, the abrasive cylinder, adjustable spring loaded mechanism.
- **Frame**
- **Hopper and casing**

The machine description and working principle has been described in Pondi et al (2017).

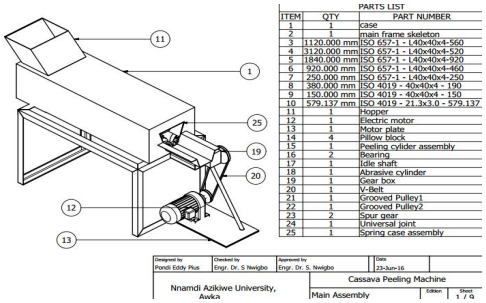

Fig. 1. Diagram of the cassava peeling machine showing all the parts [4]

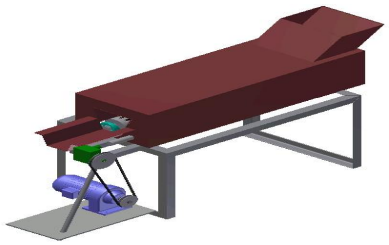

Fig. 2. 3D Model of the cassava peeling machine [4]

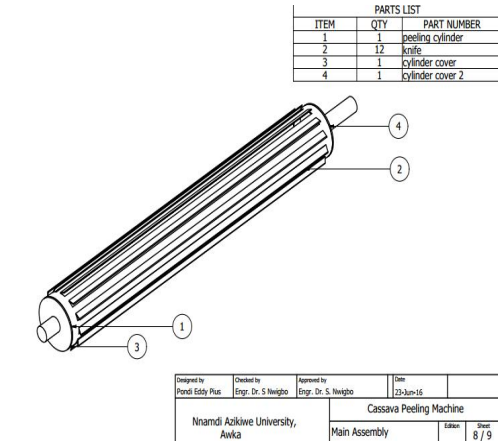

Fig. 3. Schematics of the peeling cylinder shaft

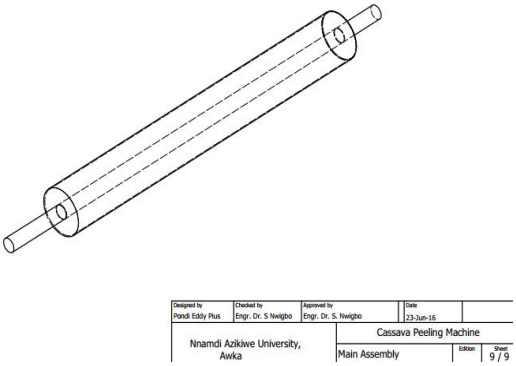

Fig. 4. Schematics of the abrasive cylinder with shaft

2.3 Design of the Components

The functional components were designed with the in-built functional design accelerator tool in Autodesk Inventor professional 2013 software while the design of other parts were done using the conventional method of design. The formulae used by the software for the calculations are based on International Standards (ISO). In addition, most of the components which are standard machine elements were selected off-the-shelf. However, emphasis on the dynamic analysis is focused on the machine shafts, to ascertain its fatigue life for safe and economic use.

2.4 Design of the Abrasive Cylinder Shaft

The abrasive cylinder shaft is subjected to a distributed load due to the weight of the abrasive cylinder, the force required to peel the cassava and the weight of the cassava.

2.4.1 Design assumptions

- There is no power loss due to mechanical coupling and friction.
- Cassava tubers will cover the entire length of the cylinder.
- The peeling force on acting on the peeling drum also acts on the abrasive cylinder.
- The peeling drum peels with one length of knife at a time.

ASME code for the design of transmission shaft subjected to torsion:

$$d^3 \frac{16}{\pi \times S_u}\left(\sqrt{(K_t M_t)^2\ (K_b M_b)^2}\right) \quad 1$$

Where, d = shaft diameter, K_t = stress shock and fatigue factor for torsion, K_b = stress shock and fatigue factor for bending, S_u = ultimate tensile strength of steel, $K_b = 1.5, K_t = 1.0$.

Fig. 5. Isometric view of the abrasive cylinder

2.4.2 Design considerations

- Power to be transmitted: 1.19KW.
- Speed of the shaft: 72 rpm.
- Torque: 0.90148 Nm.
- Distributed load from cassava tuber: 0.0493 N/mm.
- Distributed load due to the mass of the abrasive cylinder: 0.051 N/mm.
- Distributed load due to the cutting force: 0.96 N/mm.

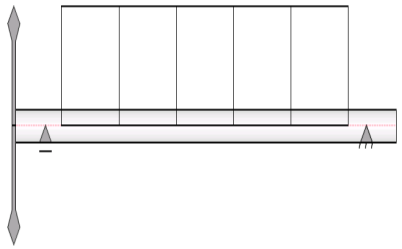

Fig. 6. Load on abrasive cylinder shaft

Table 1. Material for the abrasive cylinder shaft

Material		Steel
Modulus of Elasticity	E	206000 MPa
Modulus of Rigidity	G	80000 MPa
Density	ρ	7860 kg/m^3

Table 2. Calculation properties for abrasive shaft

S/N	Properties	Units	Calculated values
1	Density (ρ)	Kg/m^3	7860
2	Shear displacement ratio (B)	N/mm	1.188
3	Number of divisions	-	1000
4	Mode of reduced stress	N/mm	Tresca-Guest

Table 3. Loads on abrasive shaft

S/N	Location	Continuous (Size)	Continuous (Length)	Torque
1	0 mm	-	-	148N m
2	0 mm	-	-	−148 Nm
3	135 mm−945 mm	1.950 N/mm	810 mm	-

Table 4. Reaction forces on abrasive shaft

S/N	Type	Location	Reaction force
1	Free	90 mm	834.381N
2	Fixed	995 mm	825.212N

2.5 Design of Knife Cylinder Shaft

The peeling cylinder shaft is subjected to a distributed load due to the weight of the peeling cylinder, the force required to peel the cassava, and the weight of the cassava. The peeling cylinder shaft is similar to the abrasive cylinder shaft. Hence the same design assumptions are used for both shafts.

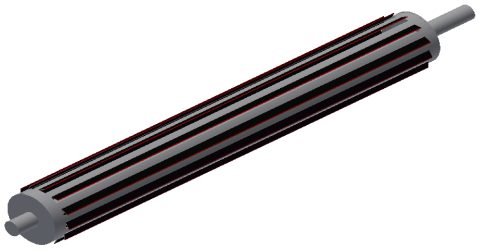

Fig. 7. Isometric view of the knife cylinder

2.5.1 Design assumptions

- There is no power loss due to mechanical coupling and friction.
- Cassava tubers will cover the entire length of the cylinder.
- The peeling force on acting on the peeling drum also acts on the peeling cylinder.
- The peeling drum peels with one length of peeling at a time.

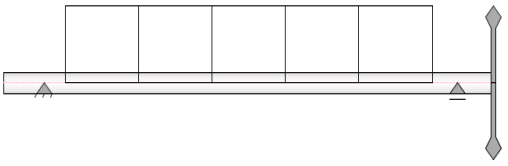

Fig. 8. Peeling cylinder shaft

Table 5. Material for peeling cylinder shaft

Material		Steel
Modulus of Elasticity	E	206000 MPa
Modulus of Rigidity	G	80000 MPa
Density	ρ	7860 kg/m^3

ASME code for the design of transmission shaft subjected to torsion:

$$d^3 \frac{16}{\pi \times S_u}\left(\sqrt{(K_t M_t)^2\ (K_b M_b)^2}\right) \quad 3.24$$

Where, d = shaft diameter, K_t = stress shock and fatigue factor for torsion, K_b = stress shock and fatigue factor for bending, S_u = ultimate tensile strength of steel, K_b = 1.5, K_t = 1.0.

2.6 Design of the Retainer Shaft

The retainer shaft is situated below the middle of the abrasive shaft cylinder and the knife cylinder shaft. Its function is to retain the cassava in the peeling zone so that it doesn't fall out. It also aids in the rotation of the cassava tuber in the peeling zone. The shaft is supported at the two ends by ball bearing. The shaft is only subjected to the distributed load from the cassava tuber which is 0.0493N/mm.

Table 6. Calculation properties for abrasive shaft

S/N	Properties	Units	Calculated values
1	Density (ρ)	Kg/m^3	7860
2	Shear displacement ratio (B)	N/mm	1.188
3	Number of divisions	-	1000
4	Mode of reduced stress	N/mm	Tresca-Guest

Table 7. Loads on abrasive shaft

S/N	Location	Continuous (Size)	Continuous (Length)	Torque
1	135 mm−945 mm	1.950 N/mm	810 mm	
2	1080 mm	-	-	148 Nm
3	1080 mm	-	-	−148 Nm

Table 8. Reaction forces on the peeling cylinder shaft

S/N	Type	Location	Reaction force
1	Fixed	90 mm	838.915N
2	Free	995 mm	820.678N

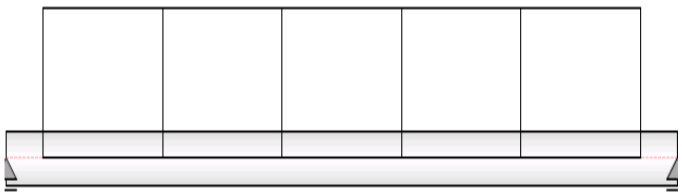

Fig. 9. Retainer shaft

Table 9. Material for the retainer shaft

Material		Stainless steel
Modulus of Elasticity	E	190000 MPa
Modulus of Rigidity	G	73000 MPa
Density	ρ	8030 kg/m^3

Table 10. Calculation properties for abrasive shaft

S/N	Properties	Units	Calculated values
1	Density (ρ)	Kg/m^3	8030
2	Shear displacement ratio (B)	N/mm	1.188

3	Number of divisions	-	1000
4	Mode of reduced stress	N/mm	Tresca-Guest

Table 11. Loads on abrasive shaft

S/N	Location	Continuous (Size)	Continuous (Length)	Torque
1	50 mm–860 mm	0.049 N/mm	810 mm	-

Table 12. Reaction forces on the retainer shaft

S/N	Type	Location	Reaction force
1	Free	0 mm	54.439N
2	Free	910 mm	54.439N

2.7 Methodology of Dynamic Simulation

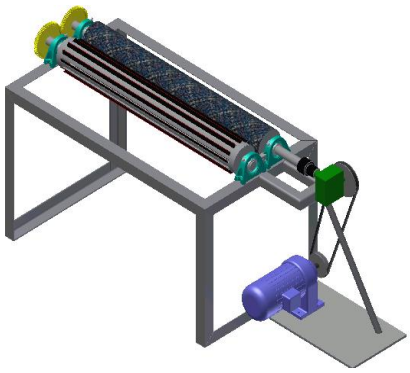

Fig. 10. View of the machine showing the rotating components

Dynamic simulations of the cassava peeling machine were carried out using Autodesk Inventor Professional Simulation Suite. The models were assembled within the assembly environment of the software before performing the simulation analysis in the dynamic simulation environment.

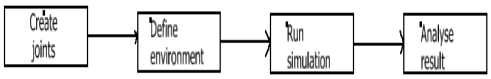

Fig. 11. Workflow in the dynamic simulation environment

2.8 Workflow in the Dynamic Simulation Environment is as Follows:

Create joints: Identify the locations where components move relative to one another. Choose the type of joint from a standard set, including pivot, spherical, point on curve contact, rolling cylinders, and others. Alternatively, convert the assembly constraints into mechanical joints. Joints are used to define the way components relate with one another during motion.

Define environment: Add physical information about the machine: Gravity, friction, damping, external forces, and others. The force and torque loads are placed on the model through the load panel and managed through the external load browser.

Run simulation: Review the motion of the model by setting up the cycle time, number of steps to show, and other items. Once the model is defined with joints and loads, one can run the dynamic simulation through the simulation player.

Analyze results: Plot and review information about the machine reactions as it runs, including positions, velocities and acceleration, reaction forces and torques, and driving forces. After simulation, the results of the maximum reaction forces is exported to FEA environment for stress analysis.

The peeling cylinder is considered for the dynamic simulation. The aim is to determine the effect of the peeling force on the peeling blades located on the peeling cylinder. The highest penetration force per unit length of 1.85N/mm and the load due to weight of the cassava (0.0493 N/mm) will be specified to be acting on the tip of the blade while the peeling cylinder and the abrasive cylinder runs at the speed of 100 rpm.

The Torque of 8.9 Nm is used for the simulation. This is the rated torque on the gear reduction unit. The acceleration due to gravity will also be specified, this will include the self-weight of the various components of the peeling cylinder to the loads used in running the dynamic simulation.

Table 13. Mesh settings for the static simulation

Avg. Element Size (fraction of model diameter)	0.1
Min. Element Size (fraction of avg. size)	0.2
Grading Factor	1.5
Max. Turn Angle	60 deg
Create Curved Mesh Elements	No
Use part based measure for Assembly mesh	Yes

Table 13 shows the mesh settings used for the static analysis.

After the dynamic simulation, the maximum force and torque generated were transferred to the FEA environment in the simulation software for static analysis.

3. RESULTS AND DISCUSSION

3.1 Result Summary for Abrasive Cylinder Shaft

The abrasive cylinder shaft is of steel material with Modulus of Elasticity (E) of 206000Mpa, Modulus of Rigidity (G) of 80000MPa, Density (P) 7860 kg/m^3. With free reaction force of 834.381N at 90 mm location and fixed reaction force of 825.212N at 995mm, applying Tresca-Guest Mode of reduced stress, the Shear displacement ratio (B) was calculated to be 1.188N/mm under 1000 Number of divisions which yielded the graphical results as shown in Figs. 12-19.

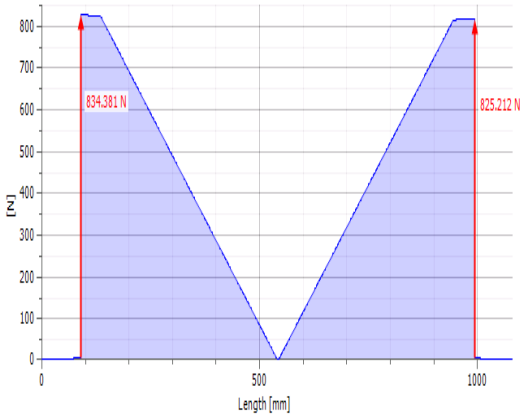

Fig. 12. Shear force diagram for abrasive cylinder shaft

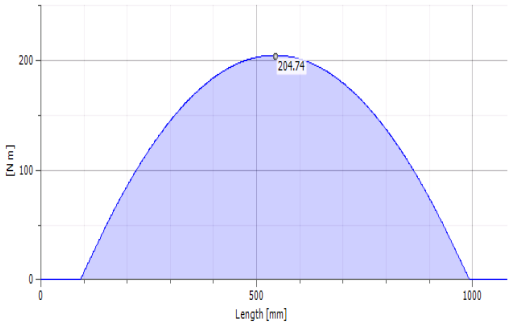

Fig. 13. Bending moment diagram for abrasive cylinder shaft

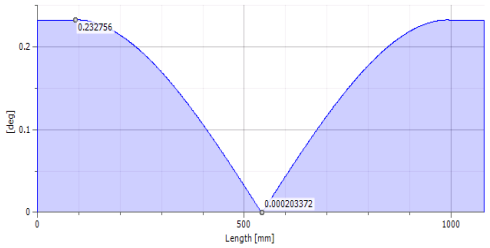

Fig. 14. Deflection angle diagram for abrasive cylinder shaft

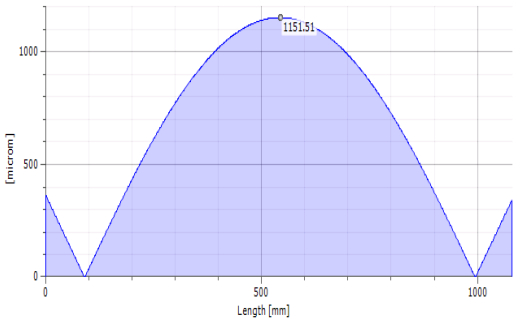

Fig. 15. Deflection diagram for abrasive cylinder

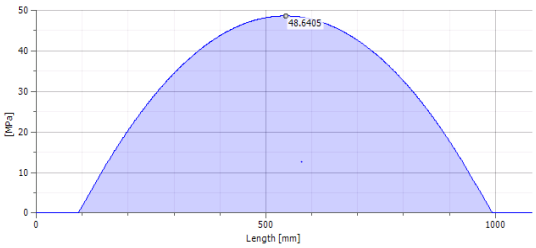

Fig. 16. Bending stress diagram for abrasive cylinder

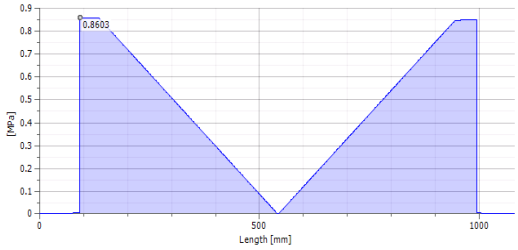

Fig. 17. Shear stress diagram for abrasive cylinder shaft

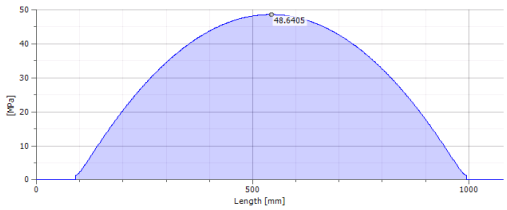

Fig. 18. Reduced stress diagram for abrasive cylinder shaft

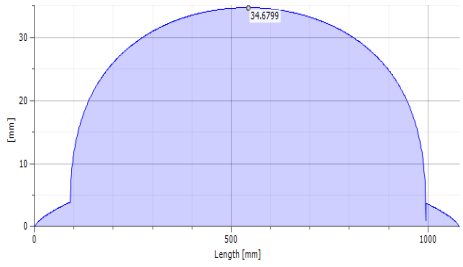

Fig. 19. Ideal diameter for abrasive cylinder shaft

From the graphs, Fig. 12 shows the shear force diagram for abrasive cylinder shaft at locations 90mm and 995mm having a reaction force of 834.331N and 825.212N respectively. Also Fig. 13 shows the bending moment diagram for the abrasive cylinder shaft, a maximum bending was noticed at 204.74Nm at locations 90 mm and 995 mm. Figs. 14 and 15 show the deflection angle diagram and deflection diagram for abrasive cylinder shaft, a maximum value of 0.232756 degree and minimum value of 0.000203372 was recorded for the deflection angle diagram of the abrasive cylinder, while a maximum value of 1151.51 microm was recorded for the deflection diagram for the abrasive cylinder. Figs. 16 and 17 show the bending stress diagram and shear stress diagram for abrasive cylinder shaft from the graph a maximum values of 48.6405MPa and 0.8603MPa was recorded for bending stress diagram and shear stress diagram for abrasive cylinder shaft respectively. Figs. 18 and 19 show the reduced stress diagram and ideal diameter for the abrasive cylinder shaft. A stress value of 48.640MPa and shaft diameter value of 34.6799 were evaluated from the reduced stress diagram and ideal diameter for abrasive cylinder shaft. Since none of stress values is greater than reduced stress (calculated stress value from Tresca's theory), the shaft will not fail in service thus a standard steel shaft of 35 mm diameter is used.

3.2 Result summary for peeling cylinder shaft

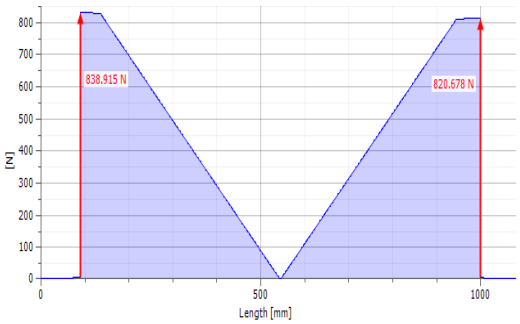

Fig. 20. Shear force diagram for peeling cylinder shaft

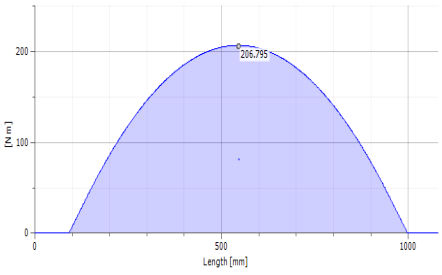

Fig. 21. Bending moment diagram for peeling cylinder shaft

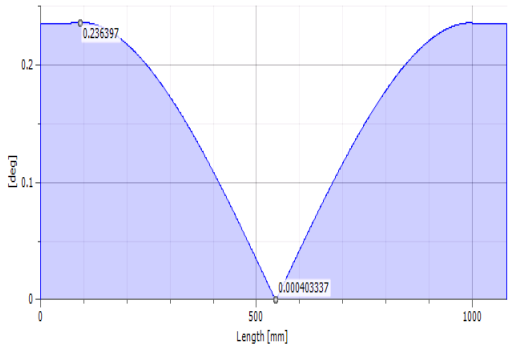

Fig. 22. Deflection angle diagram for peeling cylinder shaft

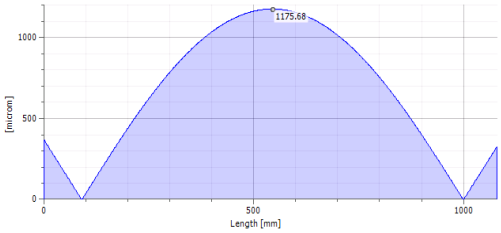

Fig. 23. Deflection diagram for peeling cylinder shaft

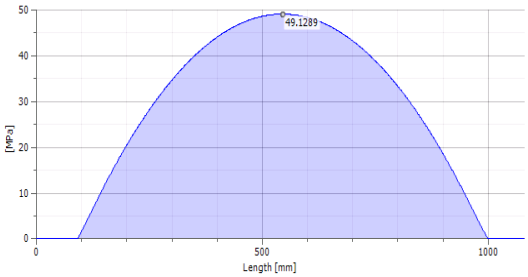

Fig. 24. Bending stress diagram for peeling cylinder shaft

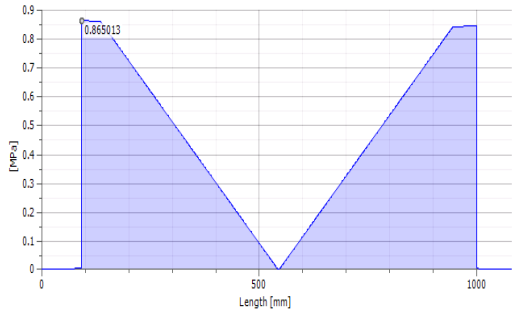

Fig. 25. Shear stress diagram for peeling cylinder shaft

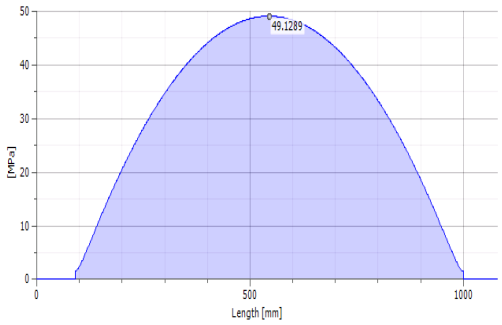

Fig. 26. Reduced stress diagram for peeling cylinder shaft

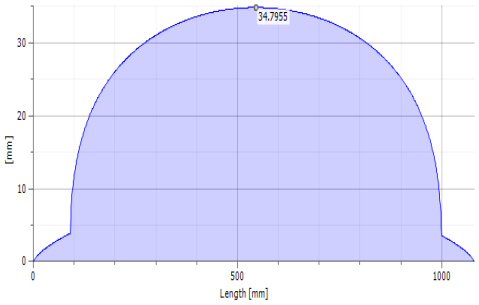

Fig. 27. Ideal diameter diagram for peeling cylinder shaft

From the graphs, Fig. 20 shows the shear force diagram for peeling cylinder shaft at locations 90 mm and 995mm having a reaction force of 838.915N and 820.678N respectively. Also Fig. 21 shows the bending moment diagram for the peeling cylinder shaft, a maximum bending was noticed at 206.795Nm at locations 90 mm and 995 mm. Figs 22 and 23 show the deflection angle diagram and deflection diagram for peeling cylinder shaft, a maximum value of 0.236397 degree and minimum value of 0.000403337 was recorded for the deflection angle diagram of the peeling cylinder shaft, while a maximum value of 1175.68 microm was recorded for the deflection diagram for the peeling cylinder shaft. Figs. 24 and 25 show the bending stress diagram and shear stress diagram for the peeling cylinder shaft. From the graph a maximum values of 49.1289 MPa and 0.865013 MPa was recorded for bending stress diagram and shear stress diagram for peeling cylinder shaft respectively. Figs. 26 and 27 show the reduced stress diagram and ideal diameter for the peeling cylinder shaft. A stress value of 49.1289 MPa and shaft diameter value of 34.7955 were evaluated from the reduced stress diagram and

ideal diameter for the peeling cylinder shaft. Since none of stress values is greater than reduced stress (calculated stress value from Tresca's theory), the shaft will not fail in service thus a standard steel shaft of 35 mm diameter is used.

3.3 Result Summary for Retainer Shaft

The retainer shaft is of steel material with Modulus of Elasticity (E) of 190000Mpa, Modulus of Rigidity (G) of 73000MPa, Density (ρ) 8030 kg/m^3. With free reaction force of 54.439N at 0 mm location and fixed reaction force of 54.439N at 910 mm, applying Tresca-Guest Mode of reduced stress, the Shear displacement ratio (B) was calculated to be 1.188N/mm under 1000 Number of divisions which yielded the graphical results as shown in Figs. 28-35.

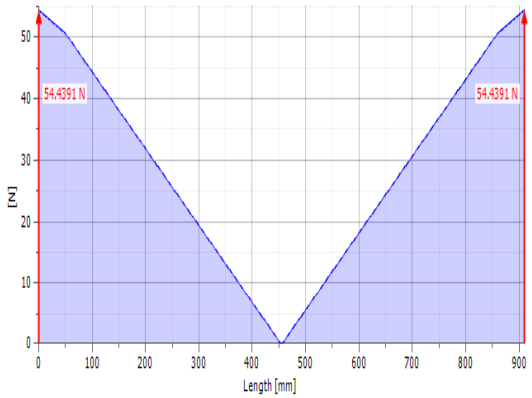

Fig. 28. Shear force diagram for retainer shaft

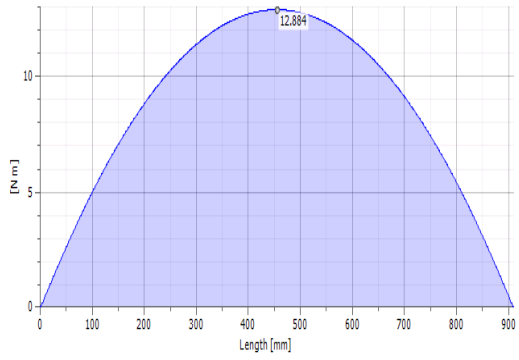

Fig. 29. Bending moment diagram for retainer shaft

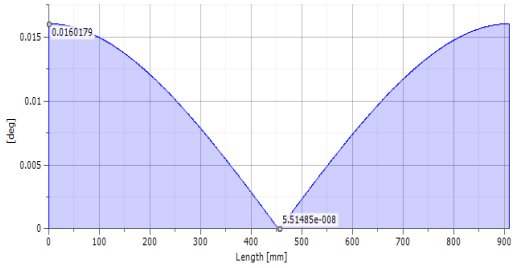

Fig. 30. Deflection angle diagram for retainer shaft

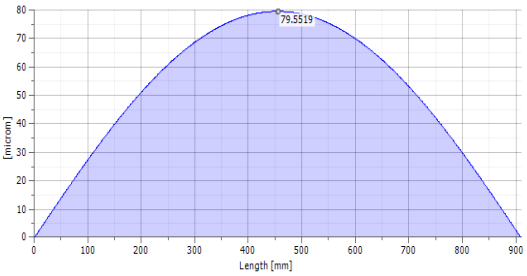

Fig. 31. Deflection diagram for retainer shaft

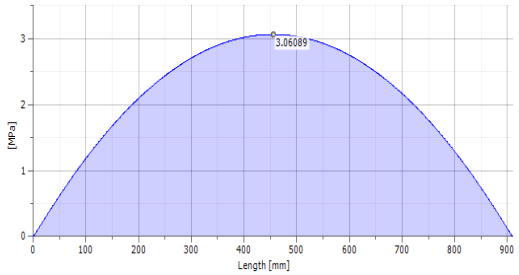

Fig. 32. Bending stress diagram for retainer shaft

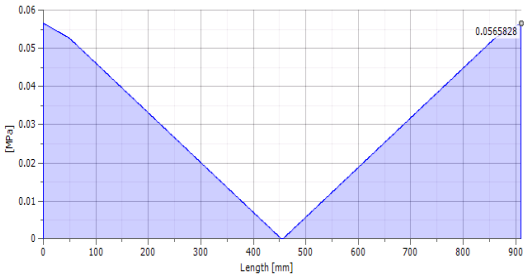

Fig. 33. Shear stress diagram for retainer shaft

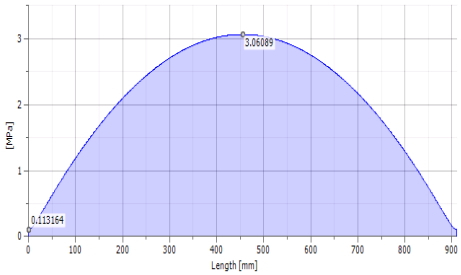

Fig. 34. Reduced stress diagram for retainer shaft

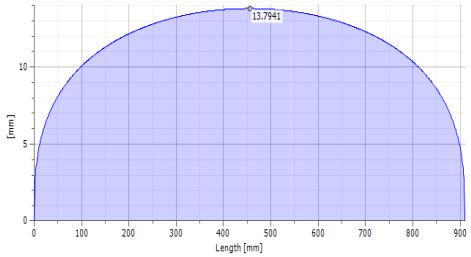

Fig. 35. Ideal diameter diagram for retainer shaft

From the graphs, Fig. 28 shows the shear force diagram for retainer shaft at locations 0 mm and 910 mm having a reaction force of 54.4391N and 54.4391N respectively. Also Fig. 29 shows the bending moment diagram for the retainer shaft, a maximum bending was noticed at 12.884Nm at locations 90mm and 995mm. Figs. 30 and 31 show the deflection angle diagram and deflection diagram for retainer shaft, a maximum value of 0.0160179 degree and minimum value of 5.51485e−008 was recorded for the deflection angle diagram of the abrasive cylinder, while a maximum value of 79.5519microm was recorded for the deflection diagram for the abrasive cylinder. Figs. 32 and 33 show the bending stress diagram and shear stress diagram for retainer shaft from the graph a maximum values of 3.06089MPa and 0.0565828MPa was recorded for bending stress diagram and shear stress diagram for retainer shaft respectively. In Figs. 34 and 35 show the reduced stress diagram and ideal diameter for retainer shaft. A stress value of 3.06089MPa and shaft diameter value of 13.7941mm were evaluated from the reduced stress diagram and ideal diameter for retainer shaft. Since none of stress values is greater than reduced stress (calculated stress value from Tresca's theory), the shaft will not fail in service thus a standard steel shaft of 35mm diameter is used.

3.4 Result Summary of Dynamic Simulation

Dynamic simulation of the cassava peeling machine were carried out using Autodesk Inventor Professional Simulation Suite. The models were assembled within the assembly environment of the software before performing the simulation analysis in the dynamic simulation environment. Figs. 34-39 shows the graphical results of the dynamic simulation. The graphs shows the acceleration of the peeling cylinder, the force acting on the peeling blade in X, Y and Z directions and the moment acting on the assembly. From the simulation, the maximum value of force is 1673.69N and the maximum value of moment is 750666Nmm at 65 seconds while the minimum value of force and moment is seen to be resident at 30 seconds. This value at 65 seconds was exported to the static analysis environment for FEA analysis.

3.5 Graphs of Dynamic Simulation Result

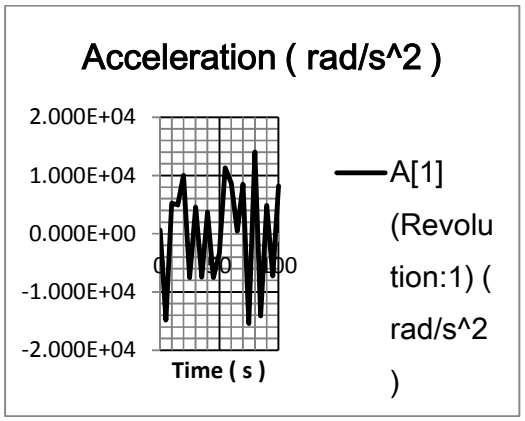

Fig. 36. Acceleration curve of the peeling cylinder

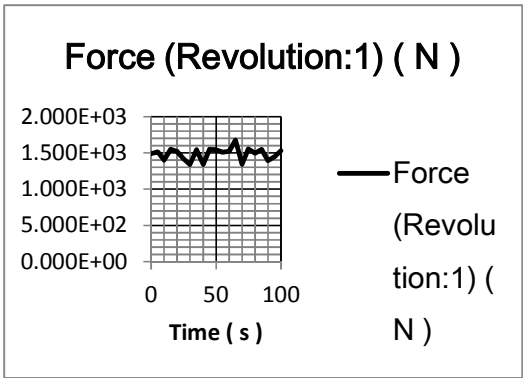

Fig. 37. Force acting on the assembly

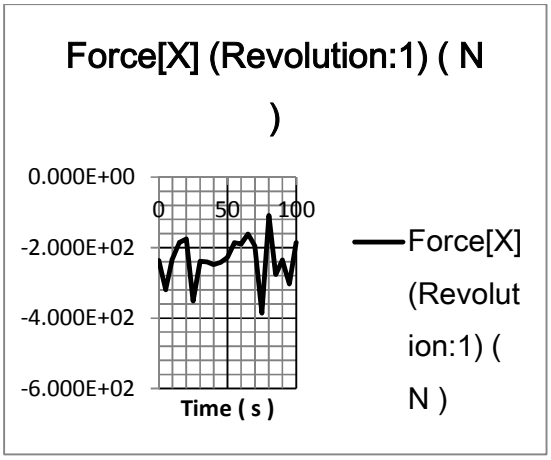

Fig. 38. Force acting on the peeling blade in X direction

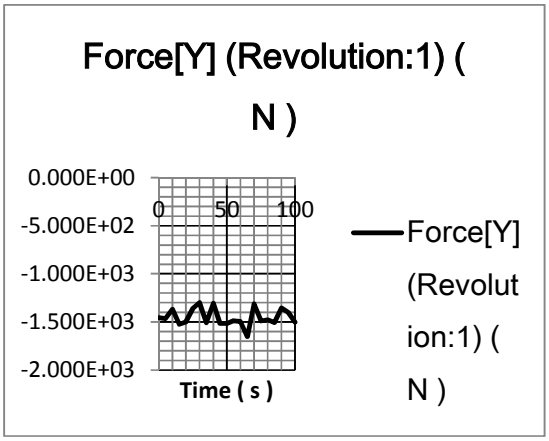

Fig. 39. Force acting on the peeling blade in Y direction

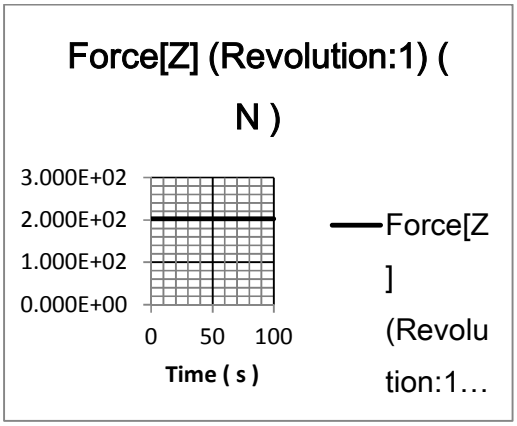

Fig. 40. Force acting on the peeling blade in Z direction

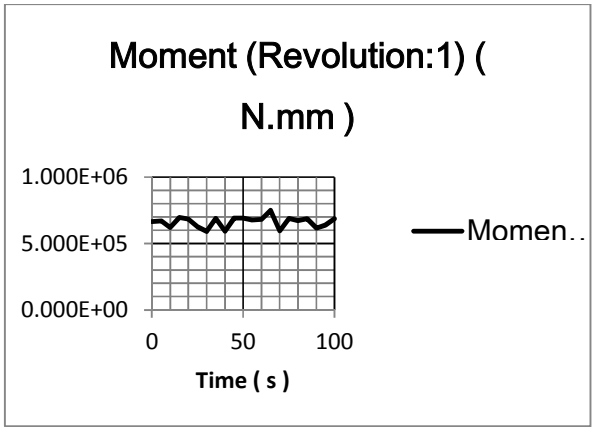

Fig. 41. Moment acting on the assembly

4. CONCLUSION

The three shafts of the cassava peeling machine have carefully analyzed to check for their fatigue life. From the analysis, with stress values of 48.640 MPa, 49.1289 MPa, 3.06089 MPa and shaft diameter values of 34.6799mm, 34.7955 mm, 13.7941 mm evaluated from the reduced stress diagrams and ideal diameter diagrams for abrasive cylinder shaft, peeling cylinder shaft, and retainer shaft respectively, gave positive results because none of stress values were greater than reduced stresses (calculated stress value from Tresca's theory) on the respective shafts. From this evaluation, it is seen that the shafts will not fail in service thus a standard steel shaft of 35 mm diameter is appropriate for manufacturing of the machine and also safe and economical.

Results of fatigue life prediction of this existing cassava peeling machine could aid design engineers in the design of more reliable and efficient cassava peeling machines to resolve the challenges of processing cost and time of production. This no doubt, will be a plus in the agro-industrial development venture of the country. This development will not only provide employment opportunities but also reduce the poverty level in the country. It will also contribute to the country's Economic Recovery and Growth Plan, which seeks to create new jobs in labour-intensive sectors like agriculture, by boosting agriculture's GDP contribution to more than 8% by 2020, up from its current levels of between 3% and 4% annually (FMARD 2012), and make the country a net exporter of cassava pellets as it holds significant export potential due to its

increasing demand in Asia, America and European market.

COMPETING INTERESTS

Authors have declared that no competing interests exist.

REFERENCES

1. Azaka Onyemazuwa Andrew, Nwadike Emmanuel Chinagorom, Umeobi Ijeoma Happiness, Ezenwa Obiora Nnaemeka. Design and analysis of a classical angular acceleration apparatus. International Journal of Multidisciplinary Sciences and Engineering. 2020;11:3. ISSN: 2045-7057.
2. Phillips TP, Taylor DS, Sanni L, Akoroda MO. A cassava industrial revolution in Nigeria; the potential for a new industrial crop. The Global Cassava Development Strategy. IFAD/ FAO, Rome; 2004.
3. Akinpelu AO, Amamgbo LEF, Olojede AO, Oyekale AS. Health Implications of Cassava Production and Consumption. Journal of Agriculture and Social Research (JASR). 2011;11:1.
4. Pondi Pius, Solomon Nwigbo. Design, fabrication, static and dynamic simulation of a cassava peeling machine. International Journal of Recent Trends in Engineering and Research (IJRTER). 2017;03(11). DOI:10.23883/IJRTER.2017.3526.YYQGL. ISSN: 2455-1457.
5. Ejovo ON, Oboli S, Mgbeke ACC. Studies and preliminary design for a cassava tuber peeling machine. Transactions of the American Society of Agric. Engineers. 1988;31(2):380-385.
6. Ohwovoriole EN, Obi S, Mgbeke ACC. "Studies and preliminary design for a cassava tuber peeling machine". Transactions of the ASAE. 1988;31(2):380-385.
7. Odigbo EU. Model III batch process cassava peeling machine presented at International Conference of Agricultural Engineering. 1983;406:88.
8. Odigboh EU. "A cassava peeling machine: Development, design and construction". Journal of Agricultural Engineering Research. 1996;21:361-369.
9. Aravie GO, Ejovo ON. Improved ohwovoriole's rotary cassava tuber peeling machine. Nigerian Journal Engineering Research and Development. 2002;1(2):61-63.
10. Adetan DA, Adekoya LO, Aluko OB, Mankanjuola GA. "An experimental mechanical cassava tubers peeling Machine. Journal of Agriculture Engineering and Technology' (JAET). 2005;13:27-34.
11. Olukunle OJ, Ogunlowo AS. Agbetoye LAS, Adesina A., Development of a self-fed cassava peeler (model A). Journal of Agricultural engineering and Environment Department of Agricultural Engineering, Federal University of Technology, Akure. 2005;39-42.
12. Agbetoye O, Oyedele A. Development and Testing of a Dual Grain Sifter. Proceeding of the Nigerian Institution of Agricultural Engineers, NIAE. 2005;192:192-193.
13. Akande FB, Adebayo AO, Busari RA. Design, fabrication and testing of manually operated cassava chipping machine. Proceedings of the Nigerian Institution of Agricultural Engineers, Adamawa. 2008;1-14.
14. Olukunle OJ, Ogunlowo OS, Sanni L. The search for effective cassava peeler. The West Indian Journal. 2010;32(1 and 2):42-47.
15. Kolawole OP, Agbetoye LAS, Ogunlowo AS., Sustaining world food security with improved cassava processing technologies: The Nigerian experience. Sustainability. 2010;2:3681-3694.

Peer-review history:
The peer review history for this paper can be accessed here:
http://www.sdiarticle4.com/review-history/66180